

# Elliptic and triangular flows in dAu collisions at 200 GeV in the fusing color string model.

M.A. Braun<sup>a</sup>, C. Pajares<sup>b</sup>

<sup>a</sup> Dep. of High Energy physics, Saint-Petersburg State University, Russia

<sup>b</sup> Dep. of Particles, University of Santiago de Compostela, Spain

September 6, 2019

## Abstract

In the color string picture with fusion and percolation the elliptic and triangular flows are studied for p-Au and d-Au collisions at 200 GeV. The ordering  $v_n(d - Au) > v_n(p - Au)$  observed experimentally for central collisions is reproduced. The calculated elliptic flow  $v_2$  at central collisions agrees satisfactorily with the data. The triangular flow  $v_3$  is found to be greater than the experimental values, similar to the results obtained in the approach based on the Color Glass Condensate initial conditions with subsequent hydrodynamical evolution.

## 1 Introduction

One of the most impressive discoveries at RHIC and LHC is observation of strong azimuthal correlations in nucleus-nucleus collisions [1, 2, 3, 4, 5, 6]. It can be characterized by the non-zero flow coefficients  $v_n$  governing the correlation function of the azimuthal distribution of secondaries as

$$C(\phi) = A \left( 1 + 2 \sum_{n=1} v_n \cos(n\phi) \right). \quad (1)$$

This effect can be understood as the formation of the fireball in the overlap of the colliding nuclei consisting of the strongly interacting hot quark-gluon plasma, which subsequently freezes, hadronises and passes into the observed secondary hadrons. The dynamics of this transition seems to be well described in the hydrodynamical approach, which relates the final spatial anisotropy to that of the initial state.

Later a similar anisotropy was observed also for collisions of smaller systems such as p-p, p-A, d-A and He-A. [7, 8, 9, 10, 11, 27, 13]. This of course has raised doubts about formation of a significantly big pieces of quark-gluon plasma in the interaction region and the subsequent hydrodynamical evolution. However calculations made within specific models of the latter [14, 15, 16] and also with initial conditions created by gluon emission in the Color Glass Condensate effective theory [17, 18, 19] seem to describe at least part of

the experimental data quite satisfactorily. So the dynamic assumptions adopted for A-A collisions seem to work also for smaller systems.

This circumstance was earlier observed in an alternative scenario for high-energy collisions, namely, the fusing color string picture. Much simpler than the hydrodynamical approach with or without previous gluon emission in the QCD framework, it allowed to describe in a satisfactory way the dependence of the spectra both on the transverse momentum and angle at various energies and for various colliding particles [20]. In this scenario the dynamics for small and big participants is qualitatively the same. The colliding nucleons form strings as soon as they are close enough and the strings then emit the observed secondary particles. The angular anisotropy in this scenario is the result of their quenching due to the presence of the gluon field from the created strings. So essentially it is a two-stage scenario as opposed to three-stage scenarios consisting first in formation of the set of interacting nucleons, then building of the initial condition ( e.g. emission of gluons) and finally the hydrodynamical expansion. Correspondingly it carries only one adjustable parameter - the universal quenching coefficient to be extracted from some data.

In this note we apply this approach to the elliptic and triangular flows  $v_2$  and  $v_3$  for p- and d-Au collisions at 200 GeV, recently measured by PHENIX [13]. It is of especial interest due to speculations that the enhanced number of primary sources in the case of d-Au collisions should lead to smaller values of  $v_2$  because the different sources (strings) are separated and do not communicate [13]. To overcome this difficulty in most recent calculations with the QCD different scales were introduced which characterize the individual domains of gluon emission; its saturation momentum and gluon resolution. Within this framework a good description of  $v_2(p_T)$  was achieved [18, 19]. As to  $v_3(p_T)$  the model overshoots the data although preserves the general trend with  $p_T$ .

As we shall find the fusing string model allows to satisfactorily describe  $v_2(p_T)$  without any additional assumptions. The triangular flow  $v_3(p_T)$  is found to lie greater than the data, as in [15] and [18, 19]. The latter authors tend to ascribe this overshooting to the details of hadronization and rescattering, which may be more important for  $v_3$ , since it is wholly fluctuation driven unlike  $v_2$ . We are working to introduce some of this effect into our model

Notice, that the glasma picture of CGC in many aspects is similar to the fusion color string model and a correspondence can be established between characteristic quantities of both approaches. The saturation momentum, occupation number and number of color flux tubes in the glasma picture correspond to to the square root of the string density, fraction of the total collision area occupied by strings and effective number of clusters of strings in the fusion of color strings approach respectively. This gives rise to the same dependence on the energy and centrality of the main observables in both approaches [21]. Thus, it is not surprising that we find similar results for the flows.

## 2 Flow coefficients in the color string model

The flow coefficients are obtained after averaging over events of the inclusive particle distribution in the azimuthal angle for a single event

$$I^e(\phi) = A^e \left[ 1 + 2 \sum_{n=1} \left( a_n^e \cos n\phi + b_n^e \sin n\phi \right) \right]. \quad (2)$$

The flow coefficients are

$$v_n = \left\langle \left[ (a_n^e)^2 + (b_n^e)^2 \right]^{1/2} \right\rangle. \quad (3)$$

In experimental observations one often uses instead of (3)

$$v_n\{2\} = \left( \left\langle (a_n^e)^2 + (b_n^e)^2 \right\rangle \right)^{1/2}. \quad (4)$$

which is somewhat greater than  $v_n$  defined by (3).

In the color string model the event is realized by a particular way of exchange of color strings between the projectile and target. Different events possess different number of strings located at different places in the overlap of the colliding nuclei. The model was proposed a long time ago to describe multiparticle production in the soft region. Its latest development and applications are described in the review paper [20]. Here we only briefly reproduce the main points necessary to understand the technique. The strings that can be visualized as drops of strong gluonic field are assumed to possess a certain finite dimension in the transverse space. Each string eventually breaks down in parts several times until its energy becomes of the order of GeV and it becomes an observed hadron. The number of strings grows with energy and atomic number and finally strings begin to overlap and fuse giving rise to clusters with more color and covering more space in the interaction area. At a certain critical density clusters acquire the transverse dimensions comparable to that of the interaction area (percolation).

It may be assumed that strings decay into particles ( $q\bar{q}$  pairs) by the well-known Schwinger mechanism for pair creation in a strong electromagnetic field.

$$P(p, \phi) = C e^{-\frac{p_0^2}{T}}, \quad (5)$$

where  $p_0$  is the particle initial transverse momentum,  $T$  is the string tension (up to an irrelevant numerical coefficient) and  $C$  is the normalization factor. To extend validity of the distribution to higher momenta one may use the idea that the string tension fluctuates, which transforms the Gaussian distribution into the thermal one [22, 23]:

$$P(p, \phi) = C e^{-\frac{p_0}{t}} \quad (6)$$

with temperature  $t = \sqrt{T/2}$ .

The initial transverse momentum  $p_0$  is thought to be different from the observed particle momentum  $p$  because the particle has to pass through the fused string areas and emit gluons on its way out. So in fact in Eq. (5) or (6) one has to consider  $p_0$  as a function of  $p$  and

path length  $l$  inside each string encountered on its way out:  $p_0 = f(p, l(\phi))$  where  $\phi$  is the azimuthal angle. It is this quenching that creates the final anisotropy and leads to nonzero flow coefficients, due to anisotropy of string distribution. To describe this quenching we use the corresponding QED picture for a charged particle moving in the external electromagnetic field [24]. This leads to the quenching formula inside a string passed by the parton [28]

$$p_0(p, l) = p \left( 1 + \kappa p^{-1/3} T^{2/3} l \right)^3, \quad (7)$$

Here  $l$  is the length traveled by the parton through the gluon fields in the hadron formed by color strings. Note that both  $l$  and  $T$  are different for different strings. When the parton passes through many strings inside the hadron one should sum different  $T_1^{2/3} l_1 + T_2^{2/3} l_2 + \dots$  over all of them. For an event both  $T_i$  and  $l_i$  are uniquely determined by the geometry of the collision and string fusion. The quenching coefficient  $\kappa$  to be taken from the experimental data. We adjusted  $\kappa$  to give the experimental value for the coefficient  $v_2$  in mid-central Pb-Pb collisions at 5-13 TeV GeV, integrated over the transverse momenta, which gives  $\kappa = 0.6$ .

Remarkably, Eq. (7) gives rise to a universal dependence of  $v_2$  on the product  $\epsilon p^{2/3} T^{1/3} l$ , where  $\epsilon$  is the eccentricity of the nuclear overlap. This scaling is well confirmed by the experimental data [25, 26]

### 3 Calculations

In the Monte-Carlo simulations of p-Au collisions at the first step one locates the interacting nucleons of the target, which are those whose distance from the projectile nucleon does not exceed two nucleon radii. For d-Au collisions one distributes the two nucleons in the deuteron according to the probability given by the deuteron wave function and locates interacting nucleons for both of them using the same criterium. For the deuteron wave function we take the Hulthen wave function. Then each pair of interacting nucleons is presented as a disk of the typical proton radius 0.8 fm and with the matter distributed inside according to the Gaussian density. The strings exchanged between them are then formed randomly distributed in the transverse plane and with the probability proportional to the hadron matter. Their number was taken from the previous calculations depending on the energy and centrality. Overlapping strings are assumed to fuse and their tension was determined from the string scenario (see [20]). Finally for a given point and direction of emission one determines the strings which the emitted particle crosses on its trajectory and lengths inside each string to find the final factor  $\sum T_i^{2/3} l_i$  entering the quenching formula. This allows to find the total probability of emission using (5) or (6) with (7). As a result one obtains the distribution in the azimuthal angle for an event and, after averaging, coefficients  $v_n$ .

Each calculation is actually done at fixed impact parameter  $b$ . To compare with the experimental data referring to most central collisions one has to take into account that the relation of  $b$  and centrality is not direct due to strong fluctuations of the number of interacting nucleons and strings at fixed  $b$  [14, 27]. To separate the contribution from a given centrality therefore one has to study the multiplicity  $\mu$  at each  $b$  and each run and select

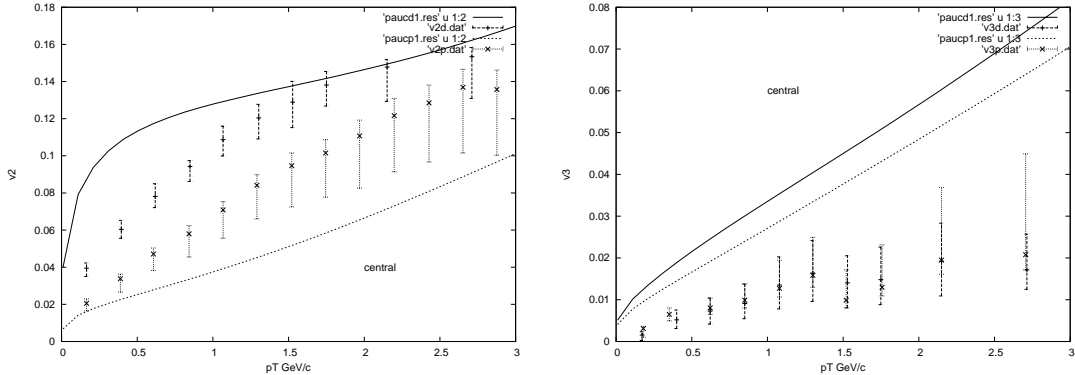


Figure 1: The calculated flow coefficients  $v_2$  (left panel) and  $v_3$  (right panel) as function of transverse momenta  $p_T$  for d-Au (upper curves) and p-Au central collisions at 200 GeV. Experimental data for  $d - Au$  (upper points) and  $p - Au$  collisions at 0-5% centrality are from [13].

events in which  $\mu$  lies within a certain part of the total interval  $\mu < \mu_{max}$  where  $\mu_{max}$  is the largest multiplicity for all  $b$  and runs. In such an approach the most central collisions can be defined as such with  $0.9\mu_{max} < \mu < \mu_{max}$ . Likewise mid-central collisions can be defined by  $0.45\mu_{max} < \mu < 0.55\mu_{max}$  and very peripheral collisions by  $\mu < 0.1\mu_{max}$ .

The results of these calculations for  $v_2$  and  $v_3$  are presented in Figs. 1-3 for  $p - Au$  and  $d - Au$  central, mid-central and peripheral collisions at 200 GeV. Comparison with the existing experimental data for central collisions [13] is shown in Fig. 1.

One has to take into account that these results were obtained by Monte-Carlo simulations with a number of runs limited by our calculational possibilities. So we estimate their statistical error as around 5%. Taking this into account we observe that our model reproduces the experimental data on  $v_2$  rather satisfactorily with some overshooting of the  $d - Au$  data and some undershooting the  $p - Au$  data. For  $d - Au$  our results for  $v_2$  resemble those of [13] although for  $p - Au$  we get somewhat lower figures. As to  $v_3$  our model gives results which substantially overshoot the data and in this respect is similar to models based on the gluonic initial conditions with the subsequent hydrodynamical evolution [17, 18, 19]. As pointed out in [18] a possible reason for this discrepancy may be related to the fact that unlike  $v_2$  the triangularity  $v_3$  is exclusively due to fluctuations and is therefore very sensitive to eventual hadronization. In our model this process is treated in a simplified way based on the well-known parton-hadron duality. We hope that a more detailed study of this stage may improve the situation.

## 4 Conclusions

An immediate consequence of our results is that they correctly describe the relative order of  $v_2$  at central collisions for  $d - Au$  and  $p - Au$  events in spite of doubts expressed in [13] and based on the comparison of the number of emitting sources in these two systems. In our

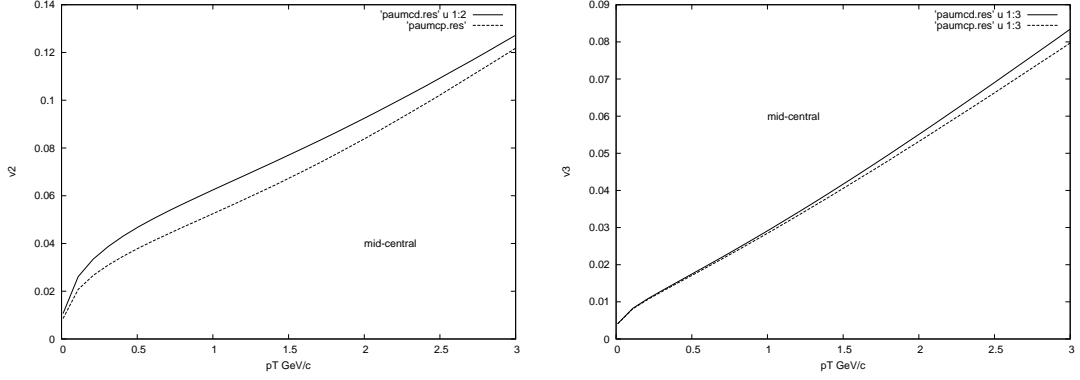


Figure 2: The calculated flow coefficients  $v_2$  (left panel) and  $v_3$  (right panel) as function of transverse momenta  $p_T$  for d-Au (upper curves) and p-Au mid-central collisions at 200 GeV.

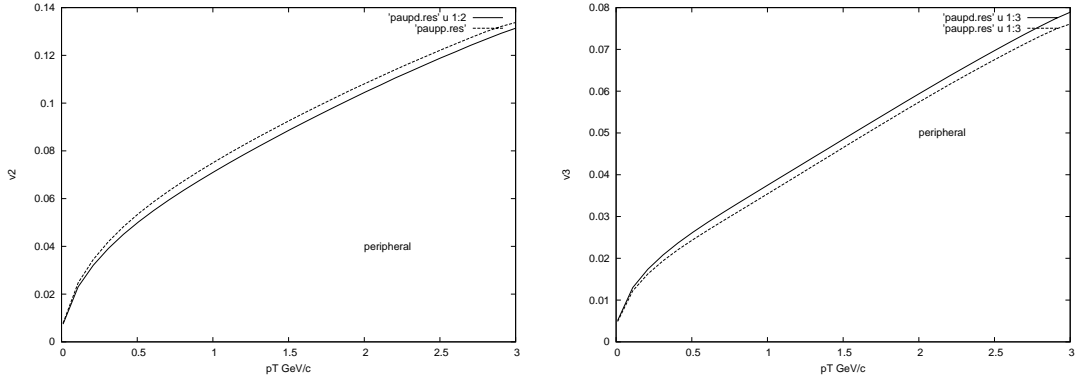


Figure 3: The calculated flow coefficients  $v_2$  (left panel) and  $v_3$  (right panel) as function of transverse momenta  $p_T$ . for d-Au and p-Au peripheral collisions at 200 GeV. For d-Au collisions  $v_2$  corresponds to the lower curve and  $v_3$  corresponds to the upper curve.

case the number of the emitting sources (strings) is naturally larger in  $d - A$  collisions than in  $p - A$  collisions (roughly twice). However they do communicate contrary to the comments in [13] by means of the commonly created gluonic field. As a result  $v_2$  for central  $d - A$  are nearly 50 % larger than for central  $p - A$  collisions.

It is interesting Figs. 2 and 3 show that this difference is diminishing with centrality and for peripheral collisions practically vanishes. This circumstance seems to be natural from pure geometrical considerations. Obviously in peripheral collisions the probability to find both of the projectile nucleons interacting with the target is minimal (if one of them interacts the other will be mostly located outside the nucleus). So the picture will not be different from  $p - Au$  collisions. The small differences in Fig. 3 should not be taken seriously due to errors involved in our Monte-Carlo simulations. It would be desirable to study this effect in the experiment.

As mentioned the triangularity  $v_3$  comes out considerably larger for both  $p - Au$  and  $d - Au$  at central collisions. In this respect our model gives results similar to the models based on the hydrodynamical evolution of the initial gluon density. We hope that some improvement of our model taking into account fluctuations in the parton-hadron conversion may improve the results for  $v_3$ . We are working on this problem.

## 5 Acknowledgements

M.A.B. appreciates hospitality and financial support of the University of Santiago de Compostela, Spain. C.P. thanks the grant Maria de Maeztu Unit of Excellence of Spain and the support Xunta de Galicia. This work was partially done under the project EPA 2017-83814-P of Ministerio Ciencia, Tecnologia y Universidades of Spain.

## References

- [1] S.Afanasiev *et al*, PHENIX collab., Phys.Rev. **C 80** (2009) 024909 [nucl-ex/0905.1070].
- [2] R.Aamodt *et al*, ALICE collab., Phys. Rev. Lett. **107** (2011) 032301 [nucl.ex/1105.3865]
- [3] A.Adare *et al*, PHENIX collab., Phys. Rev. Lett. **107** (2011) 252301 [nucl-ex/1105.3928].
- [4] B.Alver *et al* PHOBOS collab,Phys. REv. Lett. 98 (2007) 242302 [nucl-ex/0610037].
- [5] L.Adamczyk *et al* (STAR collab.), Phys. Rev. Lett. 115 (2015) 222301 [nucl-ex/1505.07812].
- [6] S Acharya *et al* (ALICE collab.) JHEP 1807 (2018) 103 [nucl-ex/1804.029442].
- [7] V.Khachatryan *et al*. JHEP **09** (2010) 091.

- [8] S.Chatrchyan *et al.* Phys.Lett. **B 718** (2013) 795.
- [9] B.Abelev *et al.* Phys.Lett. **B 719** (2013) 29.
- [10] G.Aad *et al.* Phys. Rev. Lett. **110** (2013) 182302.
- [11] A.Adare *et al.* Phys. Rev. Lett. **111** (2013) 212301.
- [12] A.Adare *et al.* Phys. Rev. Lett. **114** (2015) 192301.
- [13] C.Aidala *et al.* PHENIX collab. Nature Physics **15** (2019) 214 [ncl-ex/1805.02973].
- [14] P. Bozek,Phys. Rev. **C 85** (2012) 014911 [hep-ph/1112.0915].
- [15] M.Habich, J.L.Nagle, P.Romatschke Eur. Phys. J **C 75** (2015) 15.
- [16] C.Shen,J-F.Paquet,G.S.Denicol, S,Jeon, C.Gale, Phys. Rev. **C95** (2017) 014906.
- [17] M.Mace, V.Skokov,P.Tribedy, R.Venugopalan, Phys. Lett. **788** (2019) 161 [hep-ph/1807.00825].
- [18] M.Mace, V.Skokov,P.Tribedy, R.Venugopalan, Phys. Rev. Lett **121** (2018) 052301 [hep-ph/1805.09342]; erratum *ibid* **123** (2019) 039901.
- [19] B.Schenke, C,Shen, P.Tribedy, arXiv:1908.06212[nucl-th].
- [20] M.A.Braun, J.Dias de Deus, A.S.Hirsch, C.Pajares, R.P.Sharenberg, B.K.Srivastava, Phys. Rep., **599** (2015) 1-50.
- [21] J.Dias de Deus and C.Pajares, Phys. Lett.**B 695** (2011) 211.
- [22] A.Bialas, Phys. Lett. **B 466** (1999) 301.
- [23] J.Dias de Deus and C.Pajares, Phys. Lett.**B 642** (2006) 455.
- [24] A.I.Nikishov, Nucl. Phys. **B 21** (1970) 346.
- [25] C.Andres,J.Dias de Deus, A.Moscoso,C.Pajares, C.Salgado, Phys. Rev. **C 92** (2015) 03496.
- [26] C.Andres, M.A.Braun, C.Pajares, Eur. Phys. J. **A 53** (2017) 41.
- [27] A.Adare *et al.* PHENIX collab. Phys. Rev. **C 90** (2014) 034902.
- [28] M.A.Braun, C.Pajares, V.V.Vechernin, Nucl. Phys. **A 906** (2013) 14.